25th ABCM International Congress of Mechanical Engineering
October 20-25, 2019, Uberlândia, MG, Brazil

A SIMULATION-DRIVEN DEEP LEARNING APPROACH FOR CONDITION MONITORING OF HYDRODYNAMIC JOURNAL BEARINGS. PART II: DIAGNOSTICS OF OVALIZATION FAULTS

Ozhan Gecgel
Stephen Ekwaro-Osire
João Paulo Dias
Department of Mechanical Engineering, Texas Tech University, 805 Boston Avenue, Lubbock, TX 79409, USA
ozhan.gecgel@ttu.edu, stephen.ekwaro-osire@ttu.edu, joao-paulo.dias@ttu.edu

Gregory Bregion Daniel
Diogo Stuani Alves
Helio Fiori de Castro
School of Mechanical Engineering, University of Campinas, Rua Mendeleyev nº 200, Campinas, SP 13083-970, Brazil
gbdaniel@fem.unicamp.br, dsalves@fem.unicamp.br, heliofc@fem.unicamp.br

Abstract. *Bearings are one of the most important rotating components that play a crucial role in machine longevity. Although several studies have been done on rolling element bearings and gears, for journal bearings, it is less clear how some of the damage scenarios influence the frequency range of the measured vibration data. Moreover, most studies rely on the collection of large amounts of training data from physical experiments or from the field, which is often associated with high costs in test-rig building and instrumentation. In this paper, we developed a deep learning approach to identify ovalization faults as the second part of our research project aiming to develop condition monitoring strategies in hydrodynamic journal bearings. First, a numerical model was developed to simulate the ovalization fault conditions in order to build training datasets containing artificially generated vibration signals. Secondly, a deep learning algorithm called convolutional neural network was trained with the generated datasets and used to predict the condition of other artificially generated vibration datasets. The obtained classification accuracy results showed promising results for training the machine learning algorithms with simulated data to be later used on real applications and predictions of faults in rotating machinery.*

Keywords: *hydrodynamic journal bearing, convolutional neural network, condition monitoring, ovalization fault*

1. INTRODUCTION

Rotating machines are used in several industrial sectors, playing a relevant role in the production system. Among several elements that compose rotating machines, hydrodynamic journal bearings are one of the most important components due to their major influence on the dynamic behavior of the rotor. In this class of machines, hydrodynamic journal bearings are susceptible to different types of faults, such as cavitation, wear, and ovalization. Ovalization faults occur due to plastic deformations in the bearing profile caused by non-symmetrical heating, manufacturing uncertainty, and assembly problems, which directly affects the rotor's response (Takabi and Khonsari, 2015). The first studies which systematically investigated the dynamic behavior and hydrodynamic conditions of non-circular bearings arose during the past 30 years (Vaidyanathan and Keith Jr., 1989; Crosby, 1992; Hussain et al., 1996; Bachschmid et al., 2000). In some of these references it stated that bearing ovalization affects the second harmonic vibration component of rotating machines, which can be identified through appropriate condition monitoring and diagnostics strategies of rotating machinery. Thus, it is essential to monitor the operating conditions of these machines, in order to identify faults and conveniently plan their maintenance stops, which could potentially reduce risks of accident and economic losses.

Many researchers have studied new fault detection techniques applied to the bearing elements of rotating machines based on the machine learning and deep learning approaches (Sawalhi et al., 2014; Jeong et al., 2016; Aravazhi and Muthusamy, 2018). In most of these studies, machine health monitoring was performed throughout manual vibration signal analysis due to its excellent capability in detecting hidden fault signatures associated with machine performance. Despite the advances achieved in condition monitoring and diagnostics of rotating machinery, they still carry two major gaps. First, these works were mostly developed for applications on rolling element bearings and gears, in which specific frequencies triggered by faulty elements can be detected. For journal bearings, on the other hand, it is less clear how some of the damage scenarios (e.g. wear, ovalization) influence the frequency range of the measured vibration data (Moder et al., 2018). Secondly, and more importantly, these approaches mostly rely on the collection of large amounts of training

data from physical experiments or from the field, which is often associated with high costs in test-rig building and instrumentation (Gecgel, Ekwaro-Osire, Dias, Nispel, et al., 2019; Gecgel, Ekwaro-Osire, Dias, Serwadda, et al., 2019). The use of dynamic models to simulate the vibration response of journal bearings under many faulty conditions to create a large training dataset can be a viable alternative to the expensive collection of data from experiments or field measurements. Even using models, the generation of large training datasets is challenging due to computational power limitations to run a large number of simulations for all relevant operating condition scenarios. This issue can be solved through data augmentation of the original training dataset, which corresponds to the generation of additional new training data by applying specific deformation techniques to the original training dataset. This technique has been successfully applied in deep learning classification problems involving recognition of sounds and images (Salamon and Bello, 2017; Wang and Perez, 2017) and can be useful on problems related to fault classification in rotating machines.

Aiming to address the above-mentioned gaps, this paper presents the second part of our research project aiming to develop condition monitoring strategies in hydrodynamic journal bearings, in which a simulation-driven framework based on a deep learning algorithm to extract features and classify ovalization faults in hydrodynamic journal bearings using simulated vibration signals was proposed. First, a model to calculate the dynamic response of a journal bearing system considering the effect of bearing ovalization in the hydrodynamic lubrication regime was developed. The dynamic model was used to create a large database of simulated bearing vibration signals for several operation conditions, ovalization severities and artificially added noise levels. Lastly, a deep convolutional neural network (CNN) algorithm was implemented to classify the bearing ovalization severity using the simulated vibration signal datasets.

2. METHODOLOGY

2.1 Numerical Modeling of a Bearing with Ovalization Fault

The rotating system analyzed in this work was modeled using the Finite Element Method (FEM), considering Timoshenko's beam elements with four degrees of freedom per node, namely, two translational and two angular motions (Nelson, 1980). The equation of motion of the rotating system is given by,

$$\boldsymbol{M}\ddot{q} + (\boldsymbol{C} + \Omega\boldsymbol{G})\dot{q} + \boldsymbol{K}q = \boldsymbol{F}, \tag{1}$$

where $\boldsymbol{M}$, $\boldsymbol{C}$, $\boldsymbol{G}$ and $\boldsymbol{K}$ are global mass, damping, gyroscopic, and stiffness matrices, respectively, $\boldsymbol{F}$ is excitation force vector, q is the vector with the degrees of freedom and Ω is the angular velocity of the rotor. The hydrodynamic journal bearing model is introduced through the equivalent stiffness and damping coefficients. Thus, by applying small perturbations in the displacements and velocities of the shaft around its equilibrium position, the variation of the hydrodynamic forces can be obtained. Consequently, the equivalent stiffness and damping coefficients of the hydrodynamic bearing can be described as, (Lund, 1987):

$$K_{\mathrm{ij}} = \frac{\Delta F_{\mathrm{i}}}{\Delta e_{\mathrm{j}}}, \tag{2}$$

$$C_{\mathrm{ij}} = \frac{\Delta F_{\mathrm{i}}}{\Delta \dot{e}_{\mathrm{j}}}, \tag{3}$$

where K_{ij} and C_{ij} represent the equivalent coefficients of stiffness and damping, respectively, e is the eccentricity of the journal inside the bearing, $\dot{e}$ is the eccentricity velocity, i and j represent the XY translational directions in the cartesian reference system. The hydrodynamic forces of the bearing are obtained from the pressure distribution that is determined by Reynold's equation,

$$\frac{\partial}{\partial x}\left(h^3\frac{\partial p}{\partial x}\right) + \frac{\partial}{\partial z}\left(h^3\frac{\partial p}{\partial z}\right) = 6\mu\,\Omega\,R\frac{\partial h}{\partial x} + 12\mu\frac{\partial h}{\partial t}, \tag{4}$$

where p is the pressure distribution, μ is the dynamic viscosity of the lubricant, h is the oil film thickness, t is the time, x and z are the cartesian coordinates of the domain of the bearing. It is important to note that the Reynolds equation is solved in this work from the Finite Volume Method (Patankar, 1980) considering the central difference scheme and Gauss-Seidel iterative convergence, as used in (Silveira and Daniel, 2019). The mesh used in the numerical solution was defined after convergence tests, being composed of 51 volumes in both directions (circumferential and axial).

Once the pressure distribution is obtained, the hydrodynamic forces are calculated as,

$$F_X = \int_0^{\boldsymbol{L}}\int_0^{2\pi R} p\sin(\gamma)\,dx\,dz. \tag{5}$$

$$F_Y = \int_0^{\boldsymbol{L}}\int_0^{2\pi R} -p\cos(\gamma)\,dx\,dz. \tag{6}$$

In order to consider the fault in the bearing, the ovalization model proposed by (Silveira and Daniel, 2019) is assumed as illustrated schematically in Figure 1(a). In this model, α is the ellipticity angle, φ is the angle defined between the vertical line and the line crossing the centers of the journal and the bearing, γ is the angle of the coordinate system, and Κ is the ellipticity calculated by the difference between the maximum radial clearance and the mean radial clearance as,

$$\text{K} = C_{r_{max}} - C_r, \tag{7}$$

where $C_{r_{max}}$ is the maximum radial clearance and C_r is the mean radial clearance. Based on the oil film thickness of the elliptical bearing, the ellipse equation in polar coordinates can be described as, (Goenka and Booker, 1983)

$$R_{\text{elp}} = \frac{(C_r-\text{K})^2(C_r+\text{K})^2}{[(C_r-\text{K})\sin(\gamma)]^2+[(C_r+\text{K})\cos(\gamma)]^2}. \tag{8}$$

Assuming that $2\text{K} \ll \text{C}_\text{r} + \text{K}$, Eq. (8) can be reduced to,

$$R_{\text{elp}} = C_r - \text{K} + 2\text{K}\cos^2(\gamma) = C_r + \text{K}\cos(2\gamma). \tag{9}$$

Adding the ellipse radius to the oil film thickness of conventional journal bearings, it is possible to find the oil film thickness equation for the ovalized bearing:

$$h = C_r + e_X \sin(\gamma) - e_Y \cos(\gamma) + \text{K}\cos[2(\gamma - \alpha)]. \tag{10}$$

Figure 1(b) depicts the FEM for the bearing used in this analysis. The model consists of 16 beam elements and 1 disk element (node 11). The bearings are positioned at nodes 4 and 15. The steel shaft has an elastic modulus of 2×10^{11} N/m^2, the density of 7,850 kg/m^3, Poisson's ratio equal to 0.3, and a shear modulus equal to 0.796×10^{11} N/m^2. The coefficients of the proportional damping matrix are adjusted to 1.5×10^{-5}. Table 1 lists the bearing geometric and operation parameters considered in the simulations and the complete flowchart of the algorithm implemented for rotor-bearings system model is presented in Figure 2. The equation of motion if the rotor-bearings system is solved from the numerical time integrator. In this work, the nonlinear Newmark scheme is used along with the Newton-Raphson method in order to find the position, velocity, and acceleration values for each time step (Bathe, 2014).

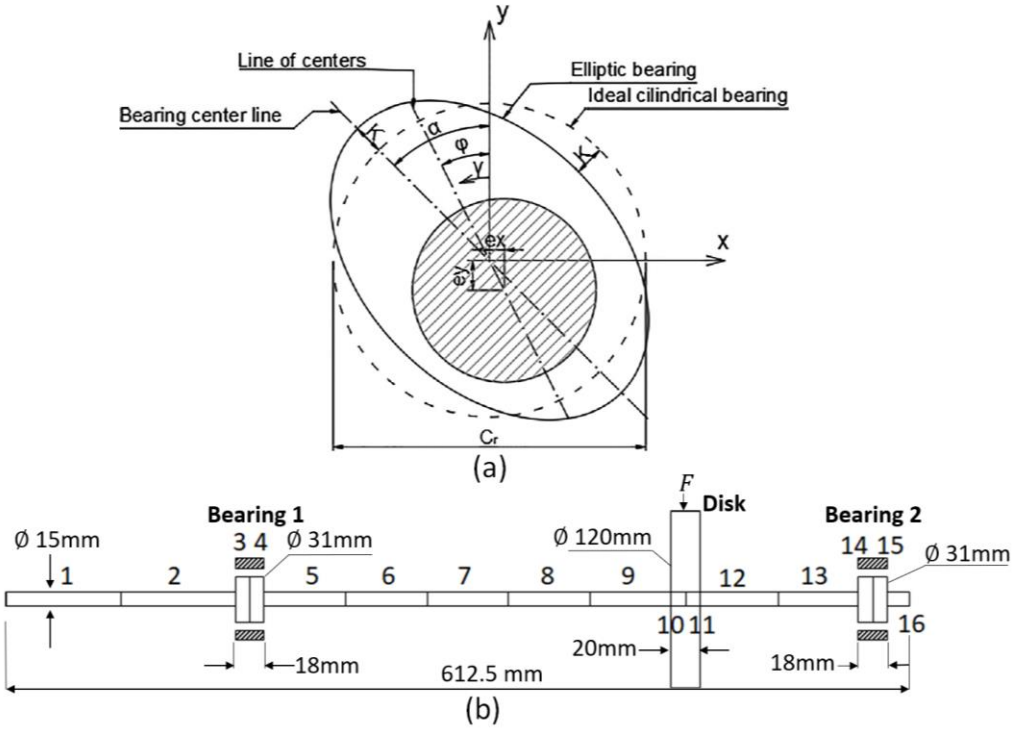

Figure 1. Models (a) Bearing model with the journal's eccentricity and other important parameters of an elliptical bearing (Silveira and Daniel, 2019) (b) Finite element model for the rotating system.

Table 1. Bearing parameters

Diameter (D)	31mm
Length (L)	20mm
Radial clearance (C_R)	90μm
Lubricant Oil	ISO VG32
Bearings loads	B1@11.31N; B2@15.94N

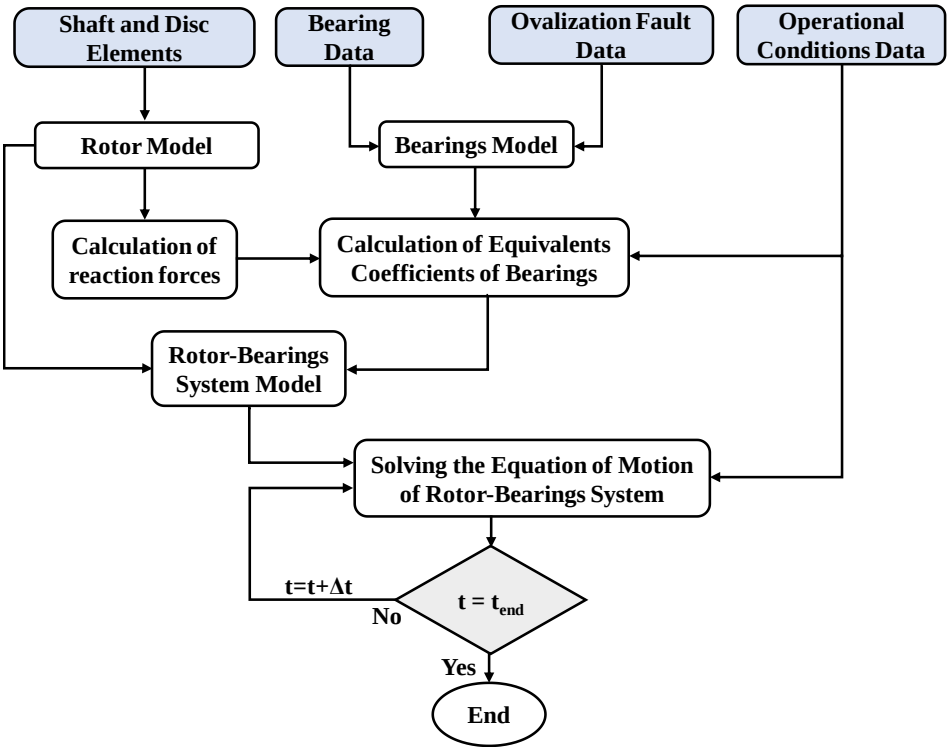

Figure 2. Flowchart of the algorithm developed for the rotor-bearings system

2.2 Fault Classification Model

For both Bearing 1 and Bearing 2, a total number of 45 signals were generated for 7 different ovalization conditions through the combination of the following operating parameters: lubricant temperature (21.5, 26.5, and 31.5°C), rotational speed (42.5, 63.75, and 85 Hz), and rotating unbalances (3.28×10^{-5}, 4.54×10^{-5}, 5.80×10^{-5}, 7.06×10^{-5}, and 8.33×10^{-5} kg.m). Therefore, a dataset with 315 vibration signals was obtained. There are many data augmentation techniques that are used to improve the results of deep learning. In order to analyze the impact of the size of the dataset, the original dataset was augmented by adding Gaussian white noise with 5 different signal-to-noise ratios (SNR) levels to the original dataset (with 10, 12, 14, 16, and 18 SNR) as shown in Figure 3. A MatLab *awgn* function was used to create augmented versions of the original dataset. All labeled signals were combined and a dataset with 270 signals per condition was obtained, which totalizes 1890 signals. Table 2 shows the dataset size of the original dataset and augmented dataset as well as the ovalization fault parameters for each condition.

Table 2. Ovalization conditions (classes) considered in the deep learning classification problem.

Ovalization Condition	Depth (μm)	Angle (°)	Original Dataset Size	Augmented Dataset Size
C1	2.7	0	45	270
C2	2.7	90	45	270
C3	5.4	0	45	270
C4	5.4	90	45	270
C5	9.0	0	45	270
C6	9.0	90	45	270
C7	0.0	-	45	270
Total number of signals			315	1890

The classification model used in this work is based on CNN. Figure 3 shows the general framework that is used in the study. After the original and augmented datasets were generated, the dataset was divided into 80% for training and 20% for testing. Each signal with its corresponding label was fed to the CNN model that consists of 3 consecutive layers of convolutional, activation and pooling, that is followed with 3 fully connected layers. After each activation layer, drop out layers were used to avoid overfitting. The testing data is fed to the trained CNN model and for each class, prediction probability is calculated and the prediction is determined with highest probability class as shown in Figure 3.

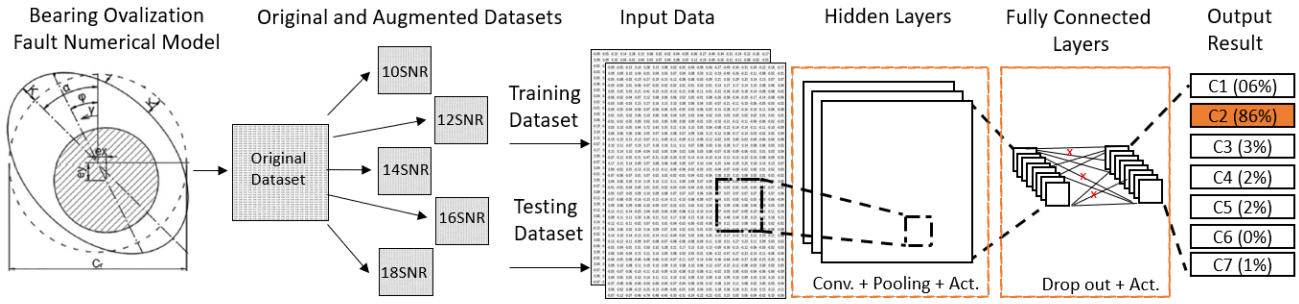

Figure 3. Ovalization fault diagnostics framework with convolutional neural network

3. RESULTS AND DISCUSSION

Figure 4(a) shows the simulated accelerations of the original dataset for the 7 conditions and Figure 4(b) shows the respective accelerations of the augmented dataset with 10 SNR noise level. For the sake of clarity in the analysis of the results, the transient part of the responses was not included in the results presented here. The original accelerations have constant amplitudes and a very regular pattern, which are not realistic according to experimental observations. In real-life situations, acceleration signals present random components due to noise, which should be taken into account in the bearing dynamic modeling. Moreover, the random nature of the added noise creates slight variations in the original signal which were used to augment the size of the training dataset.

The original dataset with 315 samples and the augmented dataset with 1,890 samples for both Bearing 1 and Bearing 2 were used as inputs to the CNN algorithm. The accuracy of the proposed ovalization fault classification framework was assessed by running the CNN algorithm 25 times consecutively with the random selection of the training and testing datasets to check the consistency and the variation of the results. The obtained results for the mean accuracies and their respective standard deviations (represented by error bars) are presented in Figure 5 for both the original and augmented datasets. One can observe that data augmentation improved the classification accuracy for both bearings. While the classification accuracy for Bearing 1 experienced a relatively slight improvement from 91% to 97%, the classification accuracy for Bearing 2 experienced a considerable improvement from 76% to 96%. Although these results seem to contradict the ones obtained in part I (Alves et al., 2019), in which the same load conditions were applied to both bearings, it is apparent that the wear and ovalization have a different impact on the fault detection capability in hydrodynamic journal bearings. The reasons for this difference will be investigated in further research.

The confusion matrices for the ovalization fault classification of Bearing 1 and Bearing 2 with the augmented datasets are presented in Figure 6(a) and (b), respectively. In this figure, the fault classification performed correctly and incorrectly can be observed in detail. The vertical axis represents the actual label of a fault condition in terms of ovalization depth and angle position, whereas the horizontal axis shows the predicted label. The diagonal of a confusion matrix (from top left to bottom right) represents the classification accuracy for each condition. A diagonal value lower than unity indicates that the classifier has confused certain ovalization condition with another one. If we consider the results in Figure 6(a), for instance, 99% of the healthy signals (C7) were predicted correctly and only 1% of these signals were misclassified as C6 (ovalization depth of 9.0 μm and angle position of 90°). In both bearings, most of the misclassification was observed in the distinction between fault conditions C2 (ovalization depth of 2.7 μm and angle position of 90°) and C4 (ovalization depth of 5.4 μm and angle position of 90°). Moreover, Bearing 2 also presented has significant misclassification rates for the fault condition C6. This trend shows that the ovalization fault positioned at 90° angle is more difficult to predict accurately, and this phenomenon needs further investigations.

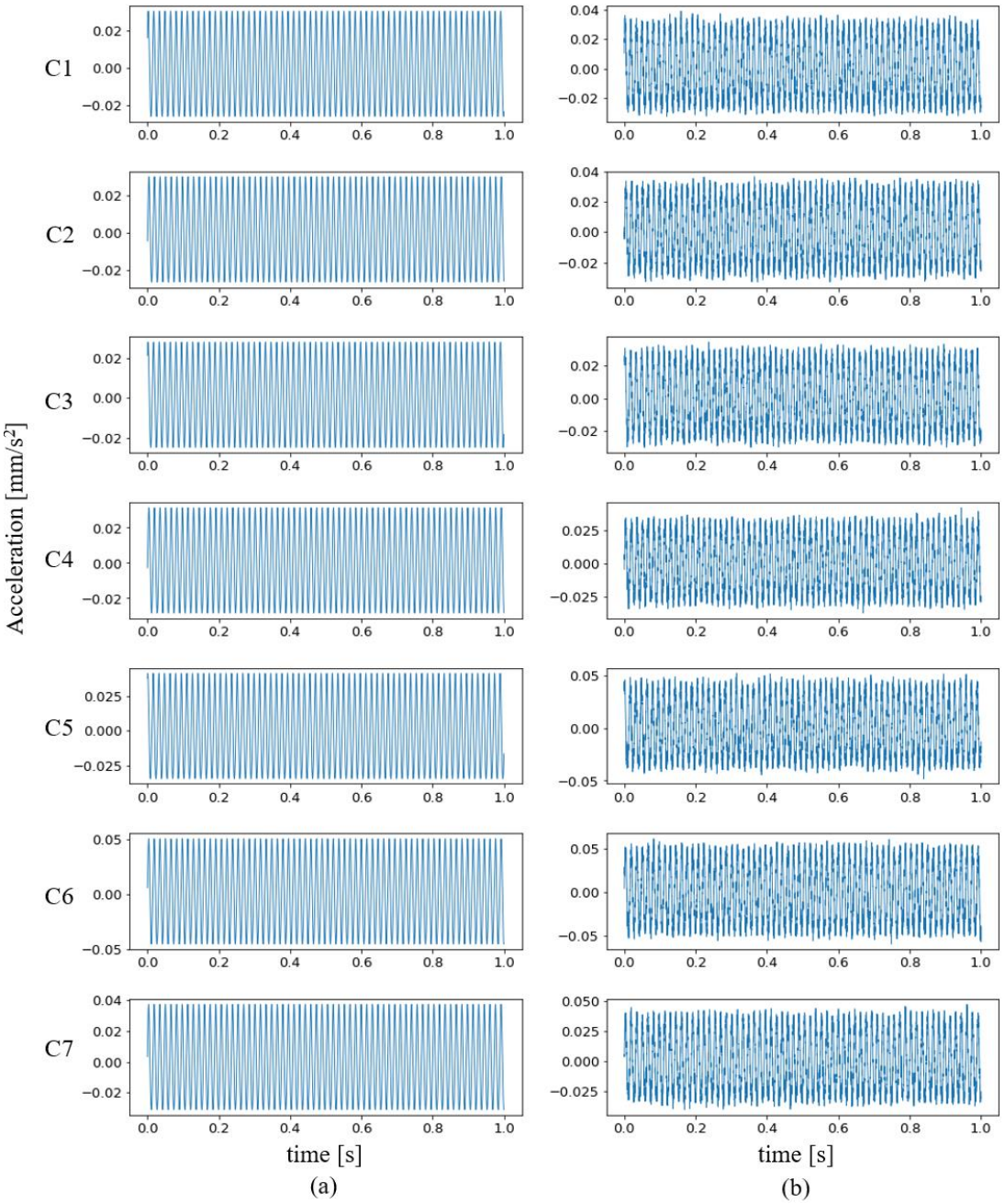

Figure 4. Simulated accelerations for seven conditions (a) without added Gaussian white noise and (b) with added Gaussian white noise (10 SNR)

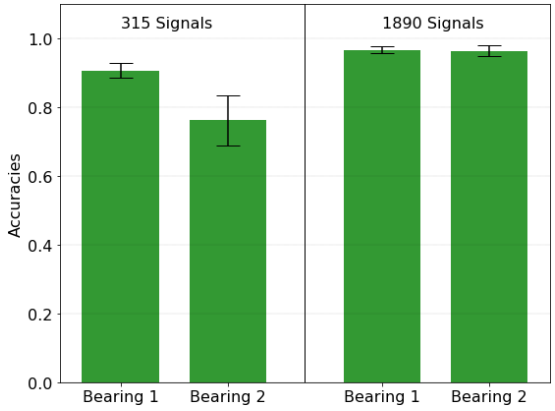

Figure 5. Accuracy results for the original and augmented dataset for Bearing 1 and 2

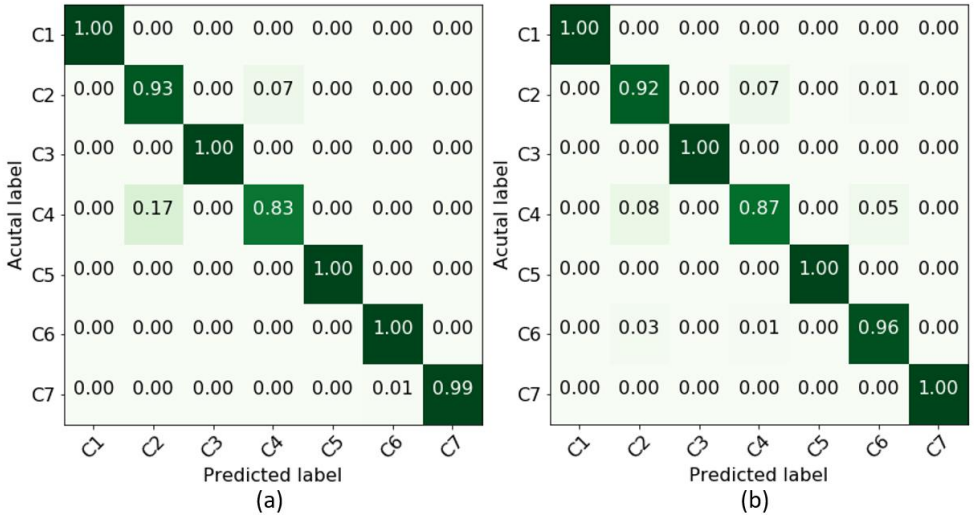

Figure 6. Confusion matrices for the ovalization fault detection for (a) Bearing 1, and (b) Bearing 2 augmented dataset

4. CONCLUDING REMARKS

In this paper, a diagnostics framework to predict ovalization faults in hydrodynamic journal bearing has been proposed using a convolutional neural network (CNN) algorithm. Bearing acceleration data was generated using a numerical model based on a coupled solution of the Reynolds Equation for the pressure distribution in the lubricant film and a finite element method to determine the dynamic response of the rotor system. Seven conditions (one for the healthy condition and 6 different faulty conditions) for 2 bearings with different static loads were simulated in order to create a baseline dataset for the fault classification. Furthermore, the baseline dataset was augmented with five different levels of Gaussian white noise in order to create a sufficiently large training dataset for the CNN algorithm. After the CNN model was trained, the testing dataset was fed to CNN and prediction accuracies were presented.

The obtained classification accuracy results showed that CNN is a powerful tool to predict ovalization faults in bearings. It was also observed that regardless of the ovalization depth, faults located at the 90° were more difficult to be correctly classified, especially at the smallest of ovalization depths. Moreover, we observed that adding different levels of Gaussian white noise to the original dataset, as a data augmentation technique, brought substantial improvements to the classification results. The obtained results demonstrate the feasibility of future applications of machine learning algorithms trained with simulated data for ovalization fault detection in real-life rotating machines.

5. ACKNOWLEDGEMENTS

The authors would like to thank São Paulo Research Foundation (FAPESP), grant 2015/20363-6, 2018/21581-5, 2019/00974-1, for the financial support to this research.

6. REFERENCES

Alves, D.S., Machado, T.H., Cavalca, K.L., Gecgel, O., Dias, J.P., and Ekwaro-Osire, S., 2019. “A Simulation-Driven Deep Learning Approach for Condition Monitoring of Hydrodynamic Journal Bearings. Part I: Diagnostics of Wear Faults.” *Proceedings of the 25th ABCM International Congress of Mechanical Engineering*. p. 1-8 (under review).

Aravazhi, A. and Muthusamy, S.M., 2018. “Machine learning based fault diagnosis of rotating machinery using sound signal,” No. May.

Bachschmid, N., Pizzigoni, B., and Tanzi, E., 2000. “On 2xrev - vibration components in rotating machinery excited by journal ovalization and oil film non-linearity.” *Proceedings of the 7th International Conference on Vibrations in Rotating Machinery*. Nottingham, U.K., p. 449–458.

Bathe, K.-J., 2014. *Finite Elment Procedures*. 2nd ed. Prentice-Hall. Englewood Cliffs, N.J.

Crosby, W.A., 1992. “An investigation of the performance of a journal bearing with a slightly irregular bore.” *Tribology International*, Vol. 25, No. 3, p. 199–204.

Gecgel, O., Ekwaro-Osire, S., Dias, J.P., Nispel, A., Alemayehu, F.M., and Serwadda, A., 2019. “Machine Learning in Crack Size Estimation of a Spur Gear Pair Using Simulated Vibration Data.” *Proceedings of the 10th International Conference on Rotor Dynamics – IFToMM Vol. 2*, Vol. 61, p. 175–190.

Gecgel, O., Ekwaro-Osire, S., Dias, J.P., Serwadda, A., Alemayehu, F.M., and Nispel, A., 2019. “Gearbox Fault Diagnostics Using Deep Learning with Simulated Data.” *Proceedings of the 2019 IEEE International Conference*

on Prognostics and Health Management. p. 1–8.
Goenka, P.K. and Booker, J.F., 1983. "Effect of Surface Ellipticity on Dynamically Loaded Cylindrical Bearings." *Journal of Lubrication Technology*, Vol. 105, No. 1, p. 1–9.
Hussain, A., Mistry, K., Biswas, S., and Athre, K., 1996. "Thermal Analysis of Noncircular Bearings." *Journal of Tribology*, Vol. 118, p. 246.
Jeong, H., Park, S., Woo, S., and Lee, S., 2016. "Rotating Machinery Diagnostics Using Deep Learning on Orbit Plot Images." *Procedia Manufacturing*, Vol. 5, p. 1107–1118.
Lund, J.W., 1987. "Review of the Concept of Dynamic Coefficients for Fluid Film Journal Bearings." *Journal of Tribology*, Vol. 109, p. 37–41.
Moder, J., Bergmann, P., and Grün, F., 2018. "Lubrication Regime Classification of Hydrodynamic Journal Bearings by Machine Learning Using Torque Data." *Lubricants*, Vol. 6, p. 108.
Nelson, H.D., 1980. "A Finite Rotating Shaft Element Using Timoshenko Beam Theory." *Journal of Mechanical Design*, Vol. 102, p. 793–803.
Patankar, S. V., 1980. *Numerical heat transfer and fluid flow*. Hemisphere Publishing Corporation. McGraw-Hill Book Company.
Salamon, J. and Bello, J.P., 2017. "Deep Convolutional Neural Networks and Data Augmentation for Environmental Sound Classification." *IEEE Signal Processing Letters*, Vol. 24, No. 3, p. 279–283.
Sawalhi, N., Gravalos, I., Pantazi, X.-E., Kateris, D., Loutridis, S., and Moshou, D., 2014. "A machine learning approach for the condition monitoring of rotating machinery." *Journal of Mechanical Science and Technology*, Vol. 28, No. 1, p. 61–71.
Silveira, A.R.G. and Daniel, G.B., 2019. "Influence of bearing ovalization in the dynamic of a planar slider-crank mechanism." *Applied Mathematical Modelling*, Vol. 66, p. 175–194.
Takabi, J. and Khonsari, M.M., 2015. "On the thermally-induced seizure in bearings: A review." *Tribology International*, Vol. 91, p. 118–130.
Vaidyanathan, K. and Keith Jr., T.G., 1989. "Numerical Prediction of Cavitation in Noncircular Journal Bearings." *Tribology Transactions*, Vol. 32, No. 2, p. 215–224.
Wang, J. and Perez, L., 2017. "The Effectiveness of Data Augmentation in Image Classification using Deep Learning." *arXiv*, Vol. 1712, No. 04621.

7. RESPONSIBILITY NOTICE

The authors are the only responsible for the printed material included in this paper.